Summary of marine sedimentary shear modulus and acoustic speed profile results using a gravity wave inversion technique

Mark V. Trevorrow[a] and Tokuo Yamamoto
Geo-Acoustics Laboratory, Division of Applied Marine Physics, Rosenstiel School of Marine and Atmospheric Science, University of Miami, 4600 Rickenbacker Causeway, Miami, Florida 33149

(Received 15 June 1990; accepted for publication 20 February 1991)

Experimental techniques and inverse methods have been established to extract marine sediment shear modulus with depth profiles from measurements of wave-induced seabed motion on the shallow continental shelf. Seabed sediments are modeled as a quasistatic, incompressible, layered elastic medium in response to wave-induced pressures. An iterative eigenvalue expansion technique is used to extract the inverse. Under typical continental shelf conditions, this inversion method is found to have a depth resolution limit of approximately 3 m, with a maximum penetration of 200 m. Using semiempirical sediment models, it is possible to deduce sediment porosity, bulk density, and shear and compressional wave speeds from the shear modulus profile. One representative result from the New Jersey Shelf is examined in detail, and favorably compared with independent sediment profiling methods. A summary of experimentally determined sediment profiles from four other sites on the Eastern U.S. continental shelf is given.

PACS numbers: 43.30.Ma

INTRODUCTION

As surface gravity water waves propagate through intermediate to shallow water (< 100 m deep), they induce small motions of the seabed sediments through variations in hydrodynamic pressure on the seafloor. The layered seabed sediments can be seen to behave in a massless, incompressible, elastic manner in response to water wave-induced pressures (Yamamoto *et al.*[1–4]). Under these circumstances it is possible to predict realistically the seabed response to passing water waves if the sediment *shear modulus* at every depth is known. Conversely, through the use of geophysical inverse methods, it is possible to extract the sediment shear modulus with depth profile from measurements of seabed motion and wave-induced pressure. This new passive sediment remote-sensing method and instrumentation system has been called the bottom shear modulus profiler (henceforth BSMP).

The experimental realization of this inversion scheme in a real ocean environment has been the thrust of five years of research by the Geo-Acoustics group at the University of Miami. The basic wave/seabed interaction theories and shear modulus inversion schemes were combined into a workable method by Yamamoto and Torii.[4] Since then many improvements and extensions to the original method have been made, and over 800 h of experimental BSMP data have been collected at sites offshore of New Jersey, George's Bank, and south Florida. This paper is intended as a summary of sedimentary results obtained over the past 5 yr using the BSMP method. It is hoped that these sedimentary geoacoustic results will provide useful references for future shallow water acoustics experiments.

Among all of the elastic moduli, the shear modulus is a particularly sensitive indicator of the *skeletal* structure of a marine sediment. Shear modulus is an important parameter in many theories modeling seismic, acoustic, and surface gravity wave propagation in the ocean. Acoustic speeds in marine sediments are very important boundary conditions for shallow water acoustic propagation models. Also, a knowledge of the sediment shear strength, related to shear modulus, is essential for the proper design of offshore and coastal structures (e.g., oil platforms and breakwaters). Extracting the seabed shear modulus is a challenging geophysical problem, but once measured the shear modulus information opens many doors into geo-acoustic modeling and engineering design.

Unfortunately, many existing methods for measuring the sediment shear modulus profile, such as standard penetration boreholes or cross-hole shear wave travel-time measurements, are physically difficult and time-consuming (and thus expensive). Such methods also suffer the unavoidable problem that the act of boring, drilling, or removing the sediment can disturb the sediment framework and grain structure. This can seriously affect the measured sediment shear modulus. Active shear wave seismology has also been pursued to determine *in situ* shear modulus (e.g., Stoll *et al.*[5]). Unfortunately, using shear waves is not as successful as compressional wave seismology in the ocean because shear waves are difficult to excite in marine sediments and the necessary geophones are difficult to couple to the seabed (Brocher and Ewing,[6] Stoll *et al.*[5]). The use of seismic interface (Scholte) waves to determine sediment properties has also received some attention[7–9] but this approach is limited by the fact that the necessary forward and inverse analyses are complicated and quite involved numerically.

In contrast, the BSMP method suffers none of these problems. The instrument package is inobtrusive to the sediments, and this method yields a true *in situ* measure of shear modulus at depth without disturbing the sediment frame. Surface gravity waves are powerful, naturally occurring, and

[a] Presently at: Ocean Physics, Institute of Ocean Sciences, 9860 W. Saanich Rd., Sidney, B.C. V8L 4B2, Canada.

 0001-4966/91/070441-16$00.80

TABLE I. BSMP experimental locations, 1986–1989.

Data set	Date	Latitude (N)	Longitude (W)	Depth (m)	Instruments
AGS 86	5–28 Aug 1986	39° 28′	74° 15′	12	3
AGS 87	29–30 Aug 1987	39° 28′	74° 15′	12	7
AGS88	7–10 July 1988	39° 28′	74° 16′	12	9
AGS89	17–22 Aug 1989	39° 29′	74° 14′	12	7
AMC6009	2–3 Sept 1987	38° 51′	73° 56′	58	6
AMC6010-87	3 Sept 1987	39° 03′	73° 07′	69	2
AMC6010-88	13–14 July 1988	39° 03′	73° 07′	68	5
Geo Bank	15–18 July 1988	40° 56′	68° 18′	51	4
Key Largo	2–7 April 1988	25° 02′	80° 28′	4.5	3
Miami	21–23 Nov 1989	25° 38′	80° 07′	7.6	3

cover a reasonably wide frequency band. The water wave signal is so dominant in its frequency band that there is only negligible noise contamination from ambient seismicity. The seabed motion is not so large, however, as to induce nonelastic shear strains in the sediment. The only limitations to the BSMP method are those of uncertainty and depth resolution, which are imposed directly by the nature of ocean waves.

There have been several major experimental tests of the BSMP instruments and methods (see Table I) collecting a total of more than 800 h of BSMP data. The basic theories and methods, and some early experimental data and verifications, have already been published (Trevorrow *et al.*,[10–12] Yamamoto *et al.*[13]). In the interest of completeness, a brief summary of the basic seabed mechanics, inverse methods, and experimental techniques is given here. These methods are illuminated using experimental data from the New Jersey Shelf (AGS site, 1987), and favorably compared with independent sediment profile results. At other sites, shear wave speed profile results are compared to borehole references and other sedimentary results tabulated in an Appendix.

I. SEABED SEDIMENT MODELS

Surface gravity waves begin to cause measurable seabed displacements when they reach water depths roughly equal to their wavelength. On the shallow continental shelf, this surface gravity wave-induced seabed motion is predominant in the frequency range 40–330 mHz, depending on the water depth. From experiments conducted over 5 yr, we have found the typical seabed displacement to have a peak amplitude of the order of 0.1 mm at a frequency of 0.1 Hz (see Trevorrow *et al.*[12]).

The usual assumption in water wave theories is that the seabed is rigid and immovable. When compared to typical water depth and wavelength scales of tens to thousands of meters, a 0.1-mm displacement is safely negligible. Thus we use the familiar linear water dispersion relation

$$\omega^2 = gk \tanh(kd). \quad (1)$$

In this case the wave number k is a unique function of angular frequency ω, gravity g, and water depth d.

Figure 1 gives a schematic of the water and sediment response. The water wave is assumed to be a two-dimensional, monochromatic plane-wave propagating in the positive x direction. The sediment response has the same wavelength as the water wave, with the seabed displacement and water surface displacement 180° out of phase. The sediment response exhibits the same prograde particle motion as the water waves. The driving force for the seabed displacement is the wave-induced bottom pressure, given by

$$P = a\rho_w g/\cosh(kd), \quad (2)$$

where a is the water wave amplitude at the water surface and ρ_w is seawater density. Note that because of the $\cosh(kd)$ term, the wave-induced pressure falls off dramatically as "kd" becomes large (deeper water or higher frequency). For example, where the water depth equals the wavelength ($kd = 2\pi$) the pressure amplitude is 0.37% of the surface value.

As a first approximation, we shall assume the seabed sediments to be isotropic, lossless, and vertically stratifed (seabed properties vary only in the vertical direction). Due to the low rigidity of the sediment as compared to its skeletal bulk modulus and the bulk modulus of water, the sediment can be assumed incompressible. This amounts to assuming that the shear wave speed c_s (in the range 50–400 m/s) is very much less than the sediment compressional speed (1500–2000 m/s) and the water acoustic wave speed ($\approx$1500 m/s). Thus the deformation is due only to shearing. Because the permeability of typical marine sediments is very small and the frame structure is relatively soft, the solid frame and pore fluid are completely coupled. Also, because

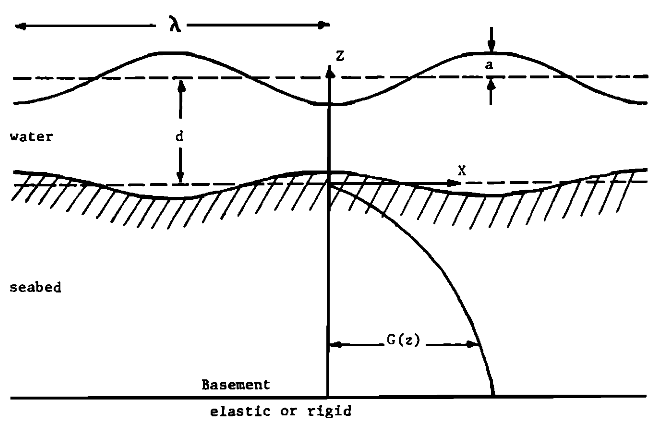

FIG. 1. Definition sketch for surface gravity wave-induced seabed motion.

water waves have a very slow propagation speed (≈ 10 m/s) as compared to that of shear waves through the sediments, inertial forces are negligible when compared with the elastic restoring forces. Furthermore, because of the small shear strains (typically 10^{-5} or less) and small amplitudes of sediment motion, nonlinearities and damping terms are quite small, and can be assumed zero if desired (Trevorrow *et al.*[10,12]). As a basic nondimensional data quantity we define horizontal (ε) and vertical (η) seabed admittance as the normalized displacements of the water–sediment interface:

$$\varepsilon = u/a, \tag{3}$$

$$\eta = w/a. \tag{4}$$

There is an unwritten harmonic phase function of $\exp[i(kx - \omega t)]$ on all disturbances. For a general, vertically stratified, isotropic seabed, the response to surface gravity waves comes from the integration of a *propagator matrix* (details given in Refs. 3, 4, 10, and 11). These matrix differential equations can be integrated numerically given any shear modulus with depth profile, a wave number, and appropriate boundary conditions. At the sediment basement, either a rigid or elastic half-space boundary condition is used (the latter more common). The boundary conditions at the water–sediment interface are that the shear stress vanishes and vertical normal stress balances bottom hydrodynamic pressure.

The shear modulus is one of the most important descriptive parameters of a marine sediment. It is a particularly sensitive indicator of the skeletal structure, as all shearing motions are transmitted only through the skeletal framework. Typical values of G for marine sediments range from 10^6 Pa for soft muds and clays to over 5×10^8 for highly consolidated sands. Another basic descriptor for a marine sediment is porosity β, which is the volume of pore space per unit volume of sediment. The typical range for porosity in marine sediments is 0.25 (highly consolidated sand) to 0.70 (muds and clays). A related parameter to porosity is the void ratio ϵ, which is the ratio of the volume of pore space to the volume of solids, and is given by

$$\epsilon = \beta/(1-\beta). \tag{5}$$

Under usual circumstances, the densities of the pore fluid and the individual grains in a marine sediment are known. The density of seawater varies only slightly about a value of 1025 kg/m^3. The sediment grains typically found on the shallow continental margins are of two types: (i) terrigenous sediments of aluminosilicate (silica, feldspar, basalt) composition, with densities close to 2600 kg/m^3 and (ii) carbonates ($CaCO_3$, shell fragments) with densities of approximately 2700 kg/m^3 or higher. We shall take an average value of 2650 kg/m^3.

With the densities of the two constituents known, and the relative proportions of each known through the porosity, we can define the bulk density by

$$\rho = \beta\rho_w + (1-\beta)\rho_s, \tag{6}$$

where the subscripts (w,s) refer to water and solid, respectively.

In the seabed the *in situ* shear modulus should increase with increasing *confining effective stress*, due to the weight of overlying sediments. We define vertical effective stress σ_z by the integral

$$\sigma_z(z) = \int_0^z g(\rho - \rho_w)\,dz, \tag{7}$$

which after substituting for bulk density and rearranging yields

$$\sigma_z(z) = g(\rho_s - \rho_w)\int_0^z 1 - \beta(z)\,dz. \tag{8}$$

Now, vertical stresses are translated to horizontal stresses through the geometry of grain-to-grain contact. Thus, we define the total effective confining stress σ as an average of the three components of effective stress, i.e.,

$$\sigma = \tfrac{1}{3}(\sigma_x + \sigma_y + \sigma_z). \tag{9}$$

Now in a horizontally stratified medium, $\sigma_x = \sigma_y$, and they are both postulated to be some fraction of the vertical stress, i.e., $\sigma_x = \sigma_y = K_0\sigma_z$. The factor K_0 is known as the *coefficient of earth pressure at rest*, and can be related to the sediment skeletal Poisson's ratio n_s by

$$K_0 = n_s/(1-n_s). \tag{10}$$

Now n_s in typical sandy and silty marine sediments can be varied in the range 0.15–0.33 (Turgut and Yamamoto[14]). We take the upper limit of 0.33 as representative, following from the fact that variations in n_s over this range cause negligible changes in the derived results. This yields K_0 equal to 1/2. Thus we can write the total effective confining stress as

$$\sigma = \tfrac{1}{3}(1+2K_0)\sigma_z = \tfrac{2}{3}\sigma_z. \tag{11}$$

A wealth of experimental data has been collected relating elastic, small strain ($<10^{-5}$) shear modulus to the depositional state of sediments (e.g., Richart *et al.*[15] and Bryan and Stoll[16]). The data indicate that the shear modulus is proportional to void ratio and total effective confining stress by an empirical relation of the form (from Yamamoto *et al.*[13])

$$G = A\epsilon^{-m}\sigma^{0.5}, \tag{12}$$

where $A = 1.835\times 10^5\sqrt{\text{Pa}}$ and $m = 1.12$. Equation (12) gives nearly identical results to empirical relations found in Bryan and Stoll.[16] This empirical relation is based on both laboratory and *in situ* seismic data from unlithified sandy, silty, or mixed-clayey sediments (β in the range 0.25–0.65). Chemical cementation effects are not considered, and thus deeper, older sediments that are slightly lithified will be *harder* (larger shear modulus) than given by this relation. In the case of cohesive clayey or muddy sediments, a more appropriate relation should be used. The reader is cautioned that laboratory values of shear modulus from clays and muds can be significantly different than *in situ* values due to plastic expansion of the core sample under release of the *in situ* confining stress (see Anderson and Woods[17]). Wherever possible, *in situ* data should be used.

Taking stock of Eqs. (5)–(12), we see that the shear modulus can be related to nothing more than a complicated function of porosity. Thus, from a knowledge of either shear modulus or porosity, the other can be calculated. In practice, the above integral [Eq. (8)] is replaced by a simple numerical integration that begins at the seafloor.

From knowledge of both the shear modulus and sediment porosity, the speeds of acoustic wave propagation in the sediment can now be estimated. The shear wave speed is straightforwardly given by

$$c_s = \sqrt{G/\rho}. \tag{13}$$

To extract the compressional wave speed we can simplify general poroelastic Biot theories. For low frequencies, the compressional wave speed is given by (following Stoll,[18] Turgut and Yamamoto[14])

$$c_c = \sqrt{H/\rho}, \tag{14}$$

where H is one of Biot's elastic moduli, related to measurable properties of the sediments by

$$H = K_s + \tfrac{4}{3}G + (K_r - K_s)^2/(D_r - K_s), \tag{15}$$

where K_r is the bulk modulus of the grain material (3.0×10^{10} Pa for silicates) and K_s is the bulk modulus of the skeletal frame, which is related to shear modulus and Poisson's ratio (both properties of skeletal frame only) via general elasticity theory, i.e.,

$$K_s = \tfrac{2}{3}[(1+n)/(1-2n)]G, \tag{16}$$

and the parameter D_r is given by

$$D_r = K_r[1 + \beta(K_r/K_f - 1)], \tag{17}$$

where K_f is the bulk modulus of the fluid component (2.31×10^9 Pa). The reader should note that the *skeletal* Poisson's ratio differs markedly from the *bulk* Poisson's ratio n_b usually determined seismically from the ratio of $c_c/c_s = \Gamma$ using the classic formula

$$n_b = (\Gamma^2 - 2)/[2(\Gamma^2 - 1)]. \tag{18}$$

Ohsaki and Iwasaki[19] report values of n_b for clayey sands and silts in the range 0.42–0.49. Hamilton[20] reports an average n_b for continental shelf sediments of 0.47. In this study, the bulk Poisson's ratios lie close to 0.48.

Obviously, the detailed results of porosity and shear and compressional wave speeds will depend on the chosen values of physical constants (e.g., ρ_s, K_r, n_s, and K_0). Fortunately, these simple models are moderately insensitive to reasonable variations in the physical constants. For example, using a skeletal Poisson's ratio of 0.15 (with a resulting change in K_0) results in a negligible ($<1\%$) change in β, ρ, and c_s, and only a 2% to 5% decrease in c_c. In practice, some *a priori* knowledge of sediment composition will enable the reader to choose appropriate physical constants. The combined uncertainties incurred from choice of physical constants and Eq. (12) ($\leqslant 5\%$) are quite small in comparison with the uncertainties in the Inversion algorithm ($\approx 40\%$).

II. INVERSE METHODS

A. Shear modulus from admittance magnitude

Knowing the shear properties of the sediments at every depth, and modeling the seabed as an incompressible, massless, layered, elastic bed, it is possible to predict accurately the seabed response to pressure forcing induced by water waves. This is a statement of the *forward* theory associated with the *inversion* process. It is possible to calculate in the *reverse* direction; to extract the shear modulus profile of the sediments from measurements of the wave-induced pressure and the seabed response (acceleration). The forward calculation is straightforward and limited only by the accuracy of the physical model and the assumptions made in deriving it. This inverse calculation, by contrast, is mathematically nonexact due to the inevitable noise in the admittance data and the fact that the water waves have only a finite frequency bandwidth.

Basically, the inverse calculation is trying to extract estimates of a continuous function (shear modulus versus depth, depth going to infinity) from a finite number of input data points (admittance) spread over a limited frequency range. The best that can be hoped for is that the finite number of data points contain enough information to sufficiently constrain any discrete estimates of the continuous function over a limited range of depths. This nonexactness manifests itself as an inherent uncertainty and resolution limit in the final result.

As is typical in geophysical problems, the relation between the shear modulus profile (model) and seabed admittance (data) is complicated and nonlinear. Because of this a linearization, iteration scheme is used to extract the inverse. The general, discrete, nonlinear relation between a vector of data parameters, $\mathbf{d}$ (M observations), and the vector of model parameters, $\mathbf{m}$ (N unknowns), can be written conceptually as

$$\mathbf{d} = f(\mathbf{m}), \tag{19}$$

where $f(\;)$ is some nonlinear functional mapping model parameters into data. To solve this inverse problem we must assume that the nonlinear function is sufficiently linear and well-behaved in a small region about the true solution, $\hat{m}$. We then expand Eq. (19) in a Taylor series about some initial value m_0

$$\mathbf{d} = f(\mathbf{m}) \approx f(\mathbf{m}_0) + \frac{\partial f(\mathbf{m})}{\partial \mathbf{m}}(\hat{m} - \mathbf{m}_0) + \cdots, \tag{20}$$

where the derivative matrix is evaluated at $\mathbf{m}_0$. We can replace $f(\mathbf{m}_0)$ with $\mathbf{d}_0$, the calculated admittance data from the initial shear modulus profile $\mathbf{m}_0$. Rearranging yields

$$\hat{m} = \mathbf{m}_0 + \left(\frac{\partial f(\mathbf{m})}{\partial \mathbf{m}}\right)^{-g}(\mathbf{d} - \mathbf{d}_0), \tag{21}$$

where the power "$-g$" denotes that we are specifying a *generalized* inverse of the derivative matrix, rather than a formal mathematical inverse. This formula is then used in an iterative fashion to cause $\mathbf{m}_0$ to creep towards $\hat{m}$. A good initial guess, $\mathbf{m}_0$, is necessary for convergence. The derivative matrix is calculated approximately using a central difference scheme. The iterations proceed until the difference between the measured and calculated admittance data is small (typically 1% rms). A detailed explanation of this inverse method is given by Trevorrow *et al.*[10] and will be only summarized here.

The generalized inverse of the derivative matrix $[\partial f(\mathbf{m})/\partial \mathbf{m}]^{-g}$ is calculated using a singular value decomposition (SVD), which performs a spectral decomposition of the derivative matrix into a set of coupled eigenvalue–eigenvector matrices. In this method, the eigensolutions corresponding to larger eigenvalues are more stable, less oscillatory, and less noise sensitive. Thus the expansion must be truncated, keeping the more stable, averaged solutions and discarding the higher-order, noisy corrections. This truncation is necessary for stability and convergence, but it is also a controlling factor in limiting the depth resolution of the final result.

B. Data and model resolution

Resolution is the ability of the method to distinguish between input data points (data resolution) or the ability to perceive small structures in the output model (model resolution). Inverse problems are characterized by their inherent limits to resolution. In this case, imperfect resolution implies that the data points are not utilized independently and that the resulting shear modulus profiles are depth-averaged to some degree. It is necessary to quantify these resolution concepts in order to properly utilize the admittance spectral data and understand the limitations of the final result.

To quantify concepts of resolution it is convenient to make use of *model* and *data resolution matrices*, which are presented in Menke[21] and Trevorrow *et al.*[10] These matrices arise naturally from manipulation of the basic inversion Eq. (21). The matrix product of the *generalized inverse* of the derivative matrix with itself is *not* the identity matrix. It turns out, however, that the degree to which this matrix product approaches the identity matrix is a measure of resolution (i.e., diagonality of these resolution matrices is desirable).

Just as with the iterative inversion calculation, the calculation of these resolution matrices includes only the first few eigensolutions. This has a serious effect on the resolution properties of the inversion, as would be expected since some higher-order information is discarded by the truncation. It turns out that the resolution properties improve (resolution matrices become more diagonal) with keeping more terms in the eigensolution expansion. Thus there is a *trade-off* with wanting the truncation limit "L" to be as large as possible for resolution considerations and wanting "L" to be small for stability. From examination of these resolution matrices, it has been determined that the minimum depth resolution of the inverted shear modulus profile is no less than 20% of the shortest wavelength available in the admittance data set. Also, resolution degrades with depth in the sediment bed, roughly limiting the ultimate penetration to 1/2 the longest wavelength available in the admittance data.

C. Uncertainty

It is of vital importance to make an estimate of the uncertainty bound of the final shear modulus profile result. Uncertainty is derived from experimental uncertainties and noise contamination in the input data and the resolution characteristics of the inverse problem itself. We use a *model covariance matrix* (see Menke[21] and Trevorrow *et al.*[10]), simplified using the truncated SVD eigensolution expansion, to quantify the uncertainty. Higher-order eigensolutions (corresponding to smaller eigenvalues) carry with them an increasingly larger uncertainty. Obviously, restricting the expansion limit results in smaller uncertainty bounds in the final result. However, this must be balanced against the desire to retain higher-order terms to increase *resolution*. This is an example of the classic trade-off between uncertainty and resolution, as discussed by Parker[22] and Menke.[21] The uncertainty bound is taken to be ± 2 standard deviations, which assuming Gaussian statistics corresponds to a 95% confidence interval.

D. Uniqueness

Uniqueness is a subtle problem that unavoidably appears in many inverse problems. Basically, nonuniqueness occurs when the input data are of insufficient bandwidth or accuracy to constrain the model to within reasonable limits. Coen[23] showed mathematically that measurements of displacement spectra at the top of a layered half-space where *sufficient* to uniquely constrain the shear modulus with depth profile at every depth. Coen did not discuss the effects of limited data bandwidth, so his result is only a partial uniqueness proof in this context. It seems reasonable that with band-limited data a unique answer can only be extracted in a limited depth range. In the past, this shear modulus inversion method has been tested for uniqueness and convergence using both numerical and real data sets. Given any particular vertical admittance data set this method has been found to produce the same final shear modulus profile, to within the quoted experimental uncertainty, from any reasonable initial guess. Each of the experimental shear modulus profile results presented in this paper has also been tested for uniqueness by trying the inversion with several different shapes and magnitudes of initial profile.

III. INSTRUMENTATION AND EXPERIMENTS

The BSMP instrument packages, in both analog and digital radio-telemetry formats, are the products of five years of experience and improvements. The measurement system consists of two separate housings connected by a 2-m-long umbilical cable, with connection to a surface buoy or ship for real-time recording. The seismometer housing is a small aluminum alloy cylinder (diam = 30.5 cm, height = 25.5 cm) designed to contain three orthogonally mounted seismometers (either Teledyne–Geotech model S-510 or S-750, or Guralp CMG-3), two pendulum tiltmeters (Sperry model 02383-01), and a compass (Aanderaa model 1248). The seismometers measure acceleration along their principal axes only, and are labeled according to their direction of mounting: vertical (z), radial (x), and transverse (y).

The other housing is a similar aluminum alloy cylinder that contains electronics, serves as a support for a differential pressure sensor (either InterOcean WS200 or PME-109), and forms a junction between the 12-conductor umbilical to the seismometer housing and a main electromechanical cable connecting to a surface buoy or ship. The pressure sensors are designed specifically to measure ultra low-frequency dynamic water pressure at depths up to 200 m. The BSMP could be deployed in either of two configurations: plate mounted or buried. The buried configuration provided superior instrument/sediment coupling (see Trevorrow *et al.*[11]).

In the analog configuration, the three seismic and hydrodynamic pressure signals are relayed directly to the attending ship, where amplification, filtering and recording are done. The digital radiotelemetry BSMP configuration has the amplifiers, filters, digitizers, and FM Telemetry systems located in the electronics housing. The digitizing rate for these units is set at 4 Hz. A coaxial cable carries + 50 Vdc power to the instruments, and returns the FM digitally multiplexed signals ($\approx$5-kHz carrier) to a surface buoy, where they are then relayed via radio to the attending ship. The maximum transmission range of this system has been found to be approximately 5 km under actual ocean conditions.

Each BSMP unit produces four analog signals (V, R, T, and P), which are amplified, filtered, and then recorded on 14-channel, 0.5-in. magnetic tape. To be able to later synchronize the digital signals with their analog counterparts, it was necessary to convert the digital signals back to analog form and record them using the same FM data recorders. To enable precise synchronization, a time-code generator signal was recorded simultaneously on each tape. Each BSMP channel has its own amplifier and filter circuit. Two series second-order low-pass antialiasing filters are used, each of which has a − 3-dB point at 0.5 Hz. Each filter circuit also has two series high-pass first-order filters, with − 3-dB points at 3.86 mHz.

Shallow burial of the seismometer housing is achieved by use of a hydraulic jet burial system. Figure 2 shows a diagram of the burial apparatus. Basically, the burial system consists of a 3-pronged burial bracket that holds the seismometer housing. The pressure sensor and electronics housing is mounted outside the burial dome, and remains on the seabed during the data collection. An electro-magnetic release mechanism, controlled from the ship, uncouples the two housings from the burial dome when the unit reaches the seabed. Seawater is pumped at high pressure through the prongs of the burial bracket, causing water jets at the tips of the prongs to liquify the sediments and excavate the sediments from underneath the seismometer housing. The burial bracket and seismometer housing sink under their own weight into the sediments. After burial, the dome and bracket are hauled back to the ship so as not to interfere with the seabed motions and pressures. The BSMP units were allowed to settle into the sediments for at least a couple of hours before the start of data recording. Using the two pendulum tiltmeters mounted inside each seismometer housing, it was possible to immediately determine if the housing was buried level. If the tilt angle was more than 10°, the BSMP unit was hauled back up to the ship and redeployed.

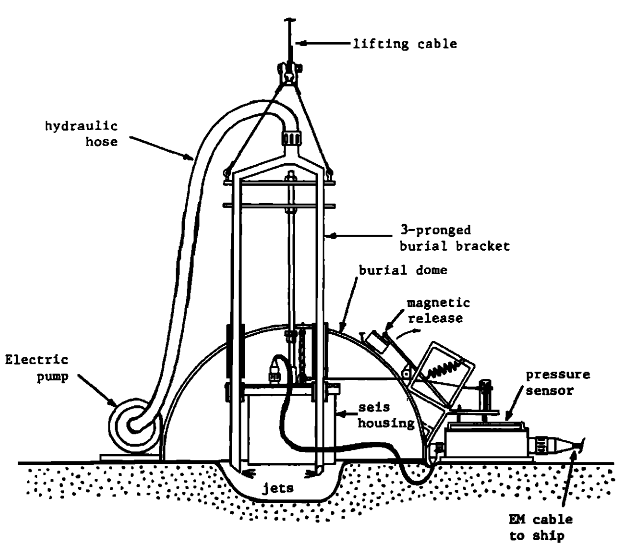

FIG. 2. BSMP burial apparatus.

IV. SPECTRAL RESULTS

The analysis of BSMP data follows standard spectral and transfer function estimation techniques. The desired input data for the shear modulus inversion method are a small number (typically 20) of vertical seabed admittance spectral components, along with their associated uncertainties. If one regards the water wave-induced seabottom pressure as an input to a linear system, and the seabed acceleration as the output, then admittance is nothing more than a *transfer function*. This necessarily requires that spectral averaging techniques be used. However, such spectral averaging must be conducted with an eye toward violations of *stationarity* in the data sets (i.e., systemic changes in sea state, wind direction, tides, etc.). The typical stationary time period has been found to be in the range 2–8 h.

The desired frequency band for this analysis is in the range 0.002–1.0 Hz, which is best suited by digitizing the raw voltage time-series at 4 Hz and using a base FFT size of 4096 points (17 minutes). This yields a Fourier spectral binwidth of 0.977 mHz. Also, a 50% overlap averaging method is used in the spectral analysis. Each time-segment is demeaned and multiplied by a 10% cosine taper window before being transformed into spectral components. The power and cross spectral components are corrected for the frequency response (magnitude and phase) of the various instruments, filters, and amplifiers. Then, we can define vertical admittance, $\eta(f)$ (complex), analogously to a transfer function from linear systems theory (from Bendat and Piersol[24])

$$\eta(f) = C(f)\,[S_{vp}(f)/S_p(f)], \tag{22}$$

where S_{vp} is the time-averaged cross-spectrum between vertical acceleration and pressure, S_p is the time-averaged pressure power spectrum, and $C(f)$ is the admittance correction factor, given by

$$C(f) = -\rho_w g/4\pi^2 f^2 \cosh(kd). \tag{23}$$

Also, it has been found convenient to use vertical seabed impedance, $I(f)$ (Pa/m), which is the ratio of sea-bottom pressure to seabed displacement. Using our previous definition of admittance this becomes

$$I_v = -4\pi^2 f^2 (S_p/S_{vp}) = \rho_w g/\cosh(kd)\eta(f). \tag{24}$$

It is also desirable to calculate the coherence parameters for the vertical admittance spectra. Coherence is a normalized magnitude of the cross spectrum, and approaches a value of 1.0 when there is a direct cause and effect relation between the two signals. Coherence is defined as

$$\gamma_v^2(f) = |S_{vp}(f)|^2/S_v(f)S_p(f). \tag{25}$$

In this case $(1-\gamma_v^2)S_v(f)$ is a measure of the noise power contaminating the vertical acceleration output. The relative

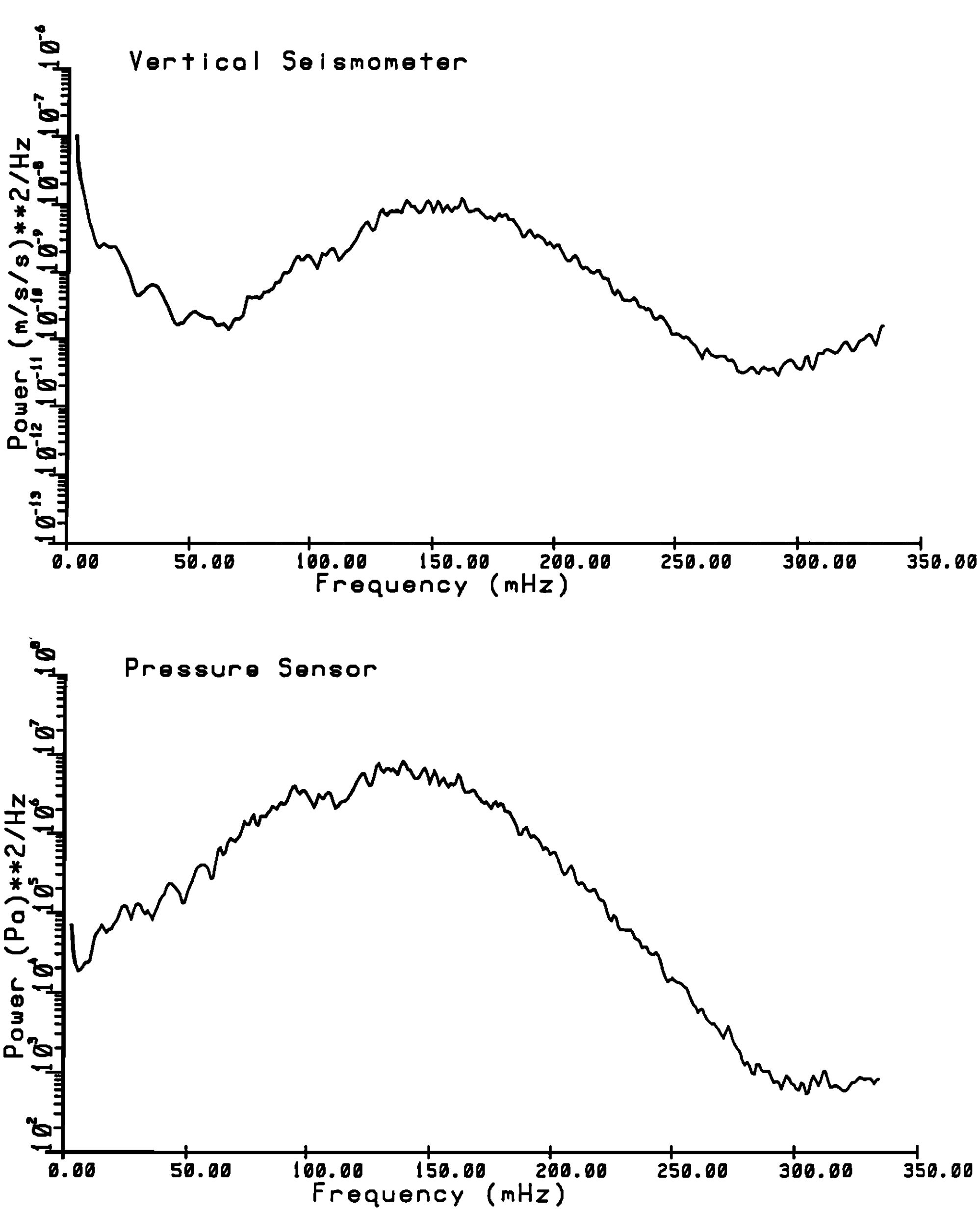

FIG. 3. Vertical acceleration and pressure power spectra from AGS site, BSMP 302 (29 Aug 1987).

error (absolute error/magnitude of spectral component) in the vertical admittance is given by (from Bendat and Piersol[24]):

$$\Delta\eta(f) = \sqrt{1-\gamma_v^2}/\gamma_v\sqrt{2N}, \tag{26}$$

where N equals the number of segments included in the spectral averaging.

At this point it is fruitful to examine some real data sets to demonstrate the results of these calculations. The example shown here is typical of the data sets collected with the BSMP instruments. Figure 3 shows the time-averaged vertical acceleration and pressure power spectra from experiments at the AGS site, BSMP 302 (29 Aug 1987). Approximately 6.5 h of data went into the calculation of these spectra. Notice the large, broad-band energy peak in the frequency range 50–275 mHz that is present in both spectra. This is due to water wave energy, mostly low-frequency *swell.* The rapid cutoff of wave energy at 170–350 mHz is due to the fact that water wave induced pressures are only significant within one wavelength of the surface, and the shorter waves do not *reach* the bottom ($\gamma = d$ at 361 mHz). In the vertical seismic spectrum, the increase in spectral levels at frequencies below 40 mHz is due to internal instrumental noise being boosted by the frequency response corrections. A more detailed discussion and summary of shallow water seabed seismicity from BSMP experiments is given in Trevorrow *et al.*[12]

Figure 4 shows the vertical seabed admittance magnitude and coherence spectra calculated from the data shown in the previous figures. The coherence parameters are plotted to identify the frequency range of good quality admittance data. Notice the range of very high coherence (≈ 0.99) in the frequency range 60–270 mHz. This very high coherence implies that there is negligible noise contamination from ambient seismicity (microseisms) in this frequency band. This is the band of good admittance data useful in the inversion process. The wider is this bandwidth of coherent data, the better will be the shear modulus inversion result.

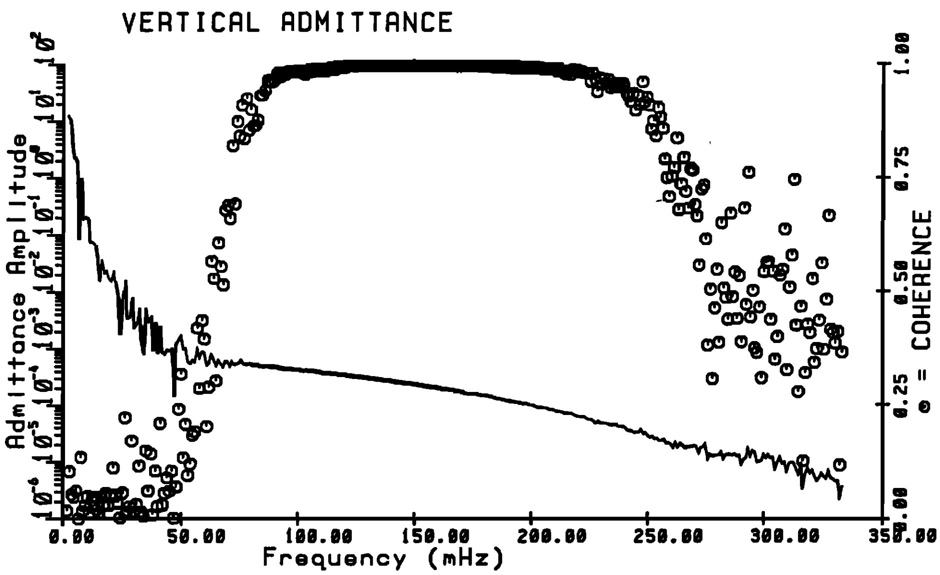

FIG. 4. Vertical admittance and coherence spectra from AGS87-302 (data shown in Fig. 3).

V. SHEAR MODULUS PROFILER RESULTS AND COMPARISONS

From the 4 yr of experiments there are over 50 distinct data sets of sufficient quality for inversion. This section will present a short selection of some of the best quality and most interesting cases. The locations for BSMP experiments (see Table I) were chosen to be in close proximity to previously conducted, independent sediment coring operations or other geophysical surveys. The sedimentary reference data come in two main forms: standard penetration test (SPT) boreholes taken at the AGS site and downhole bulk density logs taken by the AMCOR and COST drilling operations. Both can be used to calculate reference shear modulus profiles for comparison with our inverted results.

Also at the AGS and AMCOR 6009 sites, independent shear wave refraction experiments were performed by J. Ewing and G. Purdy from Wood's Hole Oceanographic Inst. and G. Sutton and J. Carter of Rondout Association. The combination of travel-time and amplitude inversions produced shear wave speed profiles that are a further comparison for the BSMP results (J. Ewing, personal communication). Details on these shear wave refraction experiments and some results are given in Stoll *et al.*[5]

Table II summarizes the experimental inversion results presented here, along with some descriptive parameters for the admittance data and the inversion result. The minimum frequency gives a measure of the deepest penetration of the inversion (roughly one-half the corresponding wavelength). The maximum frequency sets a limit to the minimum depth resolution and is strongly dependent on the water depth. The deeper sites (AMCOR 6009 and 6010) had the smallest frequency maxima. The widest frequency band (279 mHz) comes from the Miami Guralp data, due to the shallow water and improved seismometers. The smallest frequency band (81 mHz) is at the AMC6010 site, which is also the deepest water. The admittance rms relative error is a strong indicator of the quality of the data and the number of eigensolutions that may be retained. The eigensolution truncation limit L is a controlling parameter in both the resolution and uncertainty of the shear modulus result. All selected data sets could reach a truncation limit of 5, mainly because of the low admittance uncertainty levels. The mismatch error is the rms relative error between the measured and calculated admittance spectral components. The $G(z)$ error is the profile-averaged relative uncertainty in the shear modulus inversion result, which may be taken as the relative error in all derived profile results (e.g., porosity and acoustic speeds).

A. AGS site 87-302

Continuing with the example data set presented in Sec. IV, the inversion results from AGS-87 302 will now be discussed. The Atlantic Generating Station site is the survey area for a proposed offshore Nuclear Power facility, and is probably one of the most thoroughly investigated areas on the Atlantic Shelf. Stahl *et al.*[25] give a geologic description of the area. They describe three major stratigraphic units: (i) a

TABLE II. Summary of BSMP inversion results.

Data set	Depth (m)	f_{min} (mHz)	f_{max} (mHz)	Data rms error (%)	L	Mismatch error (%)	$G(z)$ error (%)
AGS-87-302	12	43.0	286.0	2.86	5	1.01	35.6
AMC6009 303	58	48.0	146.0	3.85	5	1.54	45.2
AMC6010-87 303	70	49.0	130.0	2.43	5	0.73	30.4
Geo Bank Far	51	50.0	156.0	3.98	5	1.17	28.3
Miami Guralp	7.6	91.0	370.0	2.84	5	2.48	42.3

surficial layer 2–12 m thick composed of Holocene silty and/or clayey sands, especially in the eastern sections, (ii) in the west of the site as much as 12 m of dense sand interbedded with sandy clays of late Pleistocene origin, and (iii) an underlying unit composed of Tertiary (Miocene) gravelly sands and stiff clays. The Quaternary–Tertiary (Q–T) boundary at ≈ 12 m depth is a strong acoustic reflector (Stahl *et al.*,[25] J. Ewing, personal communication).

The SPT is defined as the number of blows from a 140-lb hammer dropped through a height of 30 in. that are required to drive a 2-in.-diam sampling pipe into the sediments a distance of 1 ft. The SPT borehole data are contained in Miller and Dill.[26] An empirical relation (Ohsaki and Iwasaki[19]) gives the relation between the elastic shear modulus G and the "blow count" N as

$$G = 11.9N^{0.8}(\text{MPa}). \tag{27}$$

This relation is valid for sandy and silty sediments, but can be suspect in softer sediments where only one or two blows are required to advance the probe 1 ft. The blow-count result is useful as an indicator of the *relative* shear modulus between layers.

Figure 5 shows the inversion from selected vertical admittance spectral data shown in Figure 4. This result is a composite of two separate inversions, one penetrating to 50 m with closer spacing near the seabed surface, and the other penetrating to 100 m. The shallow inversion used admittance data in the frequency band 65–286 mHz, while the deeper inversion used a band from 43–219 mHz. The shear modulus uncertainty bound has a depth-averaged relative value of 35.6%, mostly due to larger relative uncertainties in the near surface values. The first 5 eigenvalues were included in both inversions, giving moderately good resolution characteristics. The reference profile is calculated from SPT Borehole 828 blow count result. This borehole was taken from the exact same location as this BSMP experiment, and thus is a good comparison.

Both the inversion and reference profiles clearly show the distinct Q–T boundary at 12–15 m and a softer silty-clay layer at 30 m. Notice that there is reasonable agreement be-

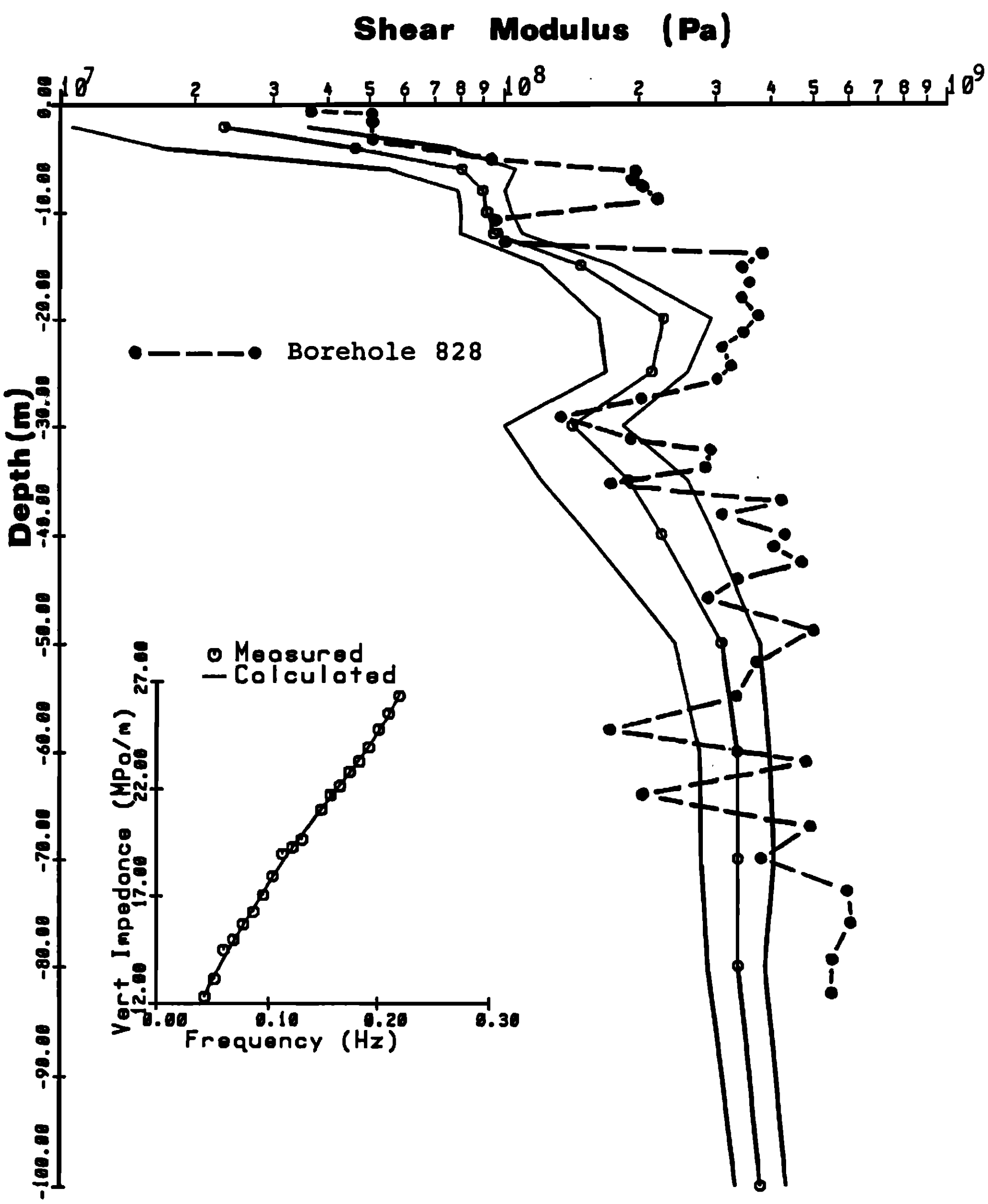

FIG. 5. Comparison of inverted shear modulus profile from AGS87-302 with reference borehole 828. Inset shows experimental versus model seabed impedance match (1.01% rms mismatch).

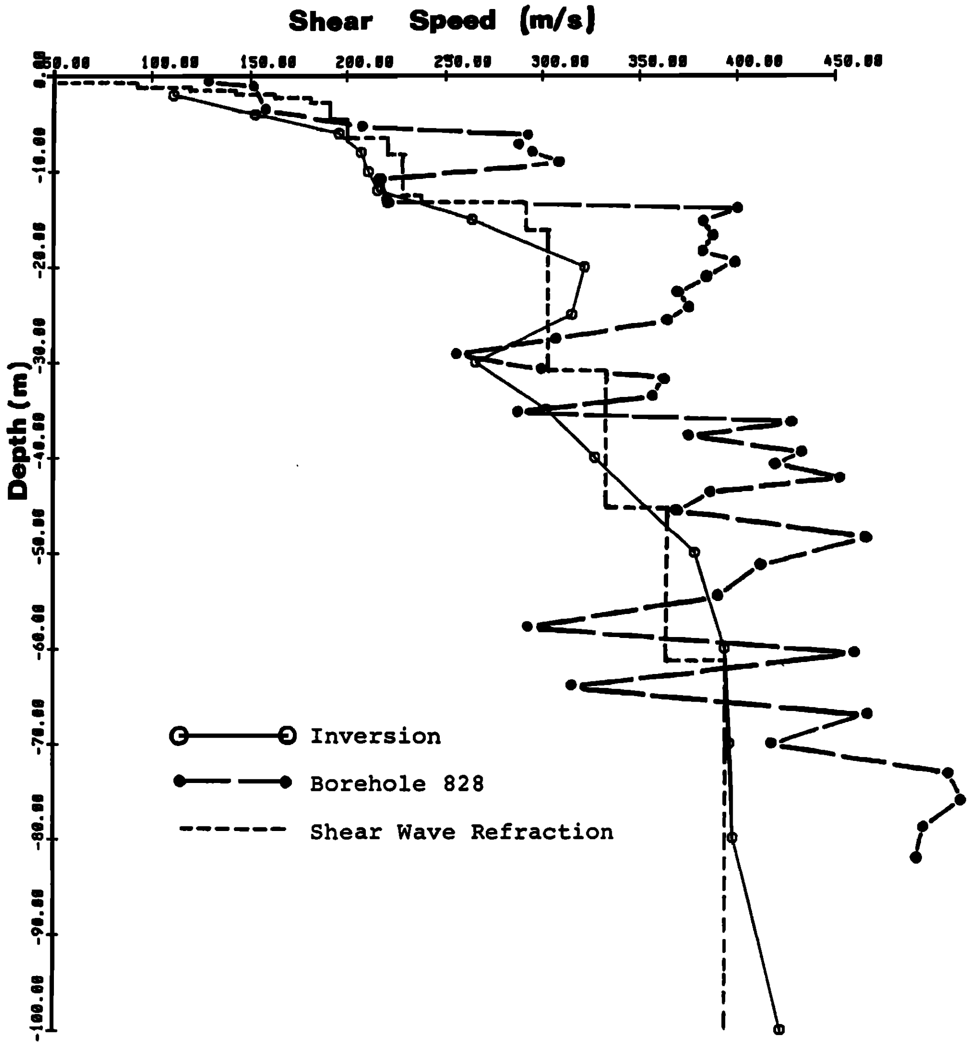

FIG. 6. Comparison of inverted shear wave speed profile from AGS87-302 (converted from shear modulus) with shear wave refraction result (from J. Ewing), and borehole 828 (converted from blow count).

tween the inversion and the reference profile at all depths, although most of the variations in shear modulus shown in the reference occur on too fine a vertical scale to be resolved by the inversion. The reference profile shows a harder layer at 5- to 8-m depth, which is only slightly indicated by the inversion.

An inset to Fig. 5 shows the 20 admittance data points, converted to vertical impedance, selected for use in the deep inversion. The uncertainty bounds on the admittance (impedance) data are of the order of 3%, and thus are not usefully shown. The calculated impedance curve fits smoothly through the data points, with a rms relative mismatch error of only 1.01%. The longest wavelength available in this data set is 254 m (at 43 mHz), so a maximum profile depth of 100 m ($\approx \frac{1}{2}\lambda_{max}$) is appropriate. The shortest wavelength is 19.1 m (at 286 mHz), which restricts the minimum resolution depth.

Figure 6 shows the shear wave profile from the inversion result compared to a shear wave refraction result from a nearby experiment, and the Borehole 828 reference converted from shear modulus. The shear wave refraction profile inversion method was restricted to strictly increasing shear wave speeds with depth to avoid triplications. All three experimental profiles show the Q–T boundary at 12 m. Note, however, that neither the BSMP inversion nor the shear wave refraction result shows the hard layer at 5–8 m indicated by the borehole reference (i.e., the blow-count result is somewhat suspect at that depth).

Figure 7 shows the porosity and compressional wave speed profiles calculated from the inversion result using the methods outlined in Sec. II. Both profiles clearly show the Q–T boundary at ≈ 12 m and the sandy clay layer at 30–35 m. The strong gradient in compressional speed at 10–15 m is the strong acoustic reflector picked up in the seismic reflection survey. The porosity value of ≈ 0.4 in the top 10 m is characteristic of silty sands, while the harder sands below 12 m have porosities of 0.25–0.3.

B. Outer New Jersey Shelf: AMCOR 6009, 6010

Two other deeper water, offshore sites on the New Jersey shelf were investigated with BSMP instruments. The Atlantic Margin Coring (AMCOR) project holes 6009 and 6010 lie in deeper waters (58 and 70 m, respectively) approximately 100 km east of the AGS site. The surficial sediments are similar to the AGS site. Both boreholes consist of sands and silty clays ranging in age from Miocene to Pleistocene (Richards,[27] Hathaway *et al.*[28]). Shear modulus inversion comparisons with converted borehole density logs at

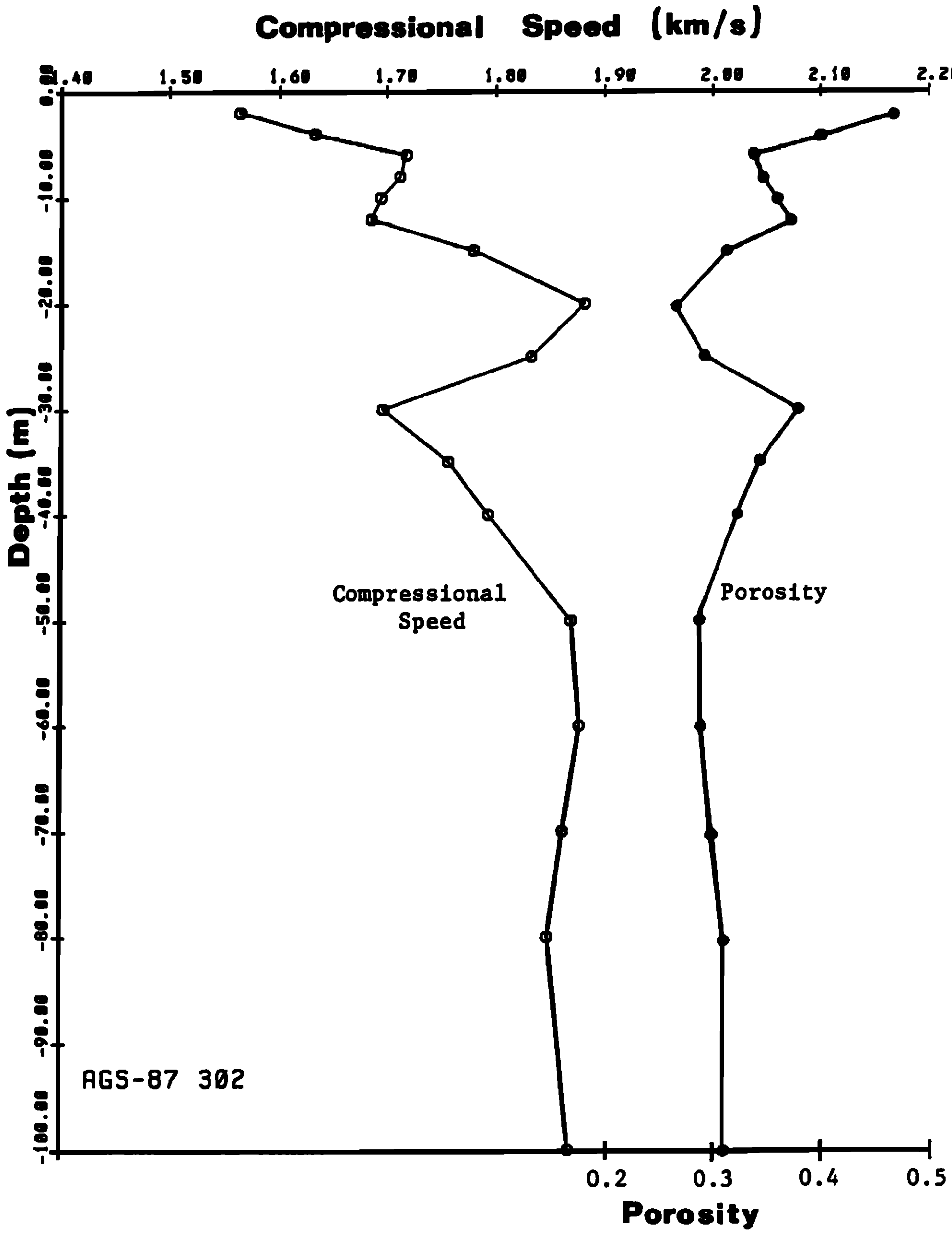

FIG. 7. Porosity and compressional speed profiles calculated from AGS87-302 shear modulus inversion.

both AMCOR 6009 and 6010 sites have been previously presented in Yamamoto *et al.*[13]

These deeper water data sets are different from the AGS site in two ways: the wavelengths at a given frequency are longer thus enabling deeper penetration (200 m), and the water depth *cut-off* limits the maximum coherent admittance data to less than 0.150 Hz. This latter problem severely limits the depth resolution of the inversion, which is no less than ≈ 20 m in both cases. Also, note from Table II that the minimum frequency of admittance data remains approximately 50 mHz for both cases. Thus, the admittance bandwidths are much narrower than at the AGS site. Figure 8 shows the shear wave speed profile (converted from shear modulus inversion) for the AMCOR-6009 site, compared to a shear wave refraction experimental profile and a reference profile calculated from the AMCOR borehole bulk density log. Owing to resolution limits,the inversion can match only the larger scale features of the borehole reference, such as the soft layer at 30–40 m, but tends to average away small scale structures. The agreement between the inversion and refraction results in the topmost 15 m is excellent. Figure 9 shows a similar shear wave speed profile comparison for the AMCOR-6010 site. Again there is good agreement with the borehole reference in a depth-averaged sense. In particular, observe the ability of the inversion to match the faster (harder) layers at 30–40 m and 90–120 m. The shear modulus inversion and derived sediment parameters from these AMCOR sites are shown in Tables AI and AII (see Appendix).

C. George's Bank

Perhaps the physically most difficult BSMP deployment was at the George's Bank site, where strong winds, seas, and tidal currents permitted only two digital BSMP units to be properly deployed. The George's Bank site has

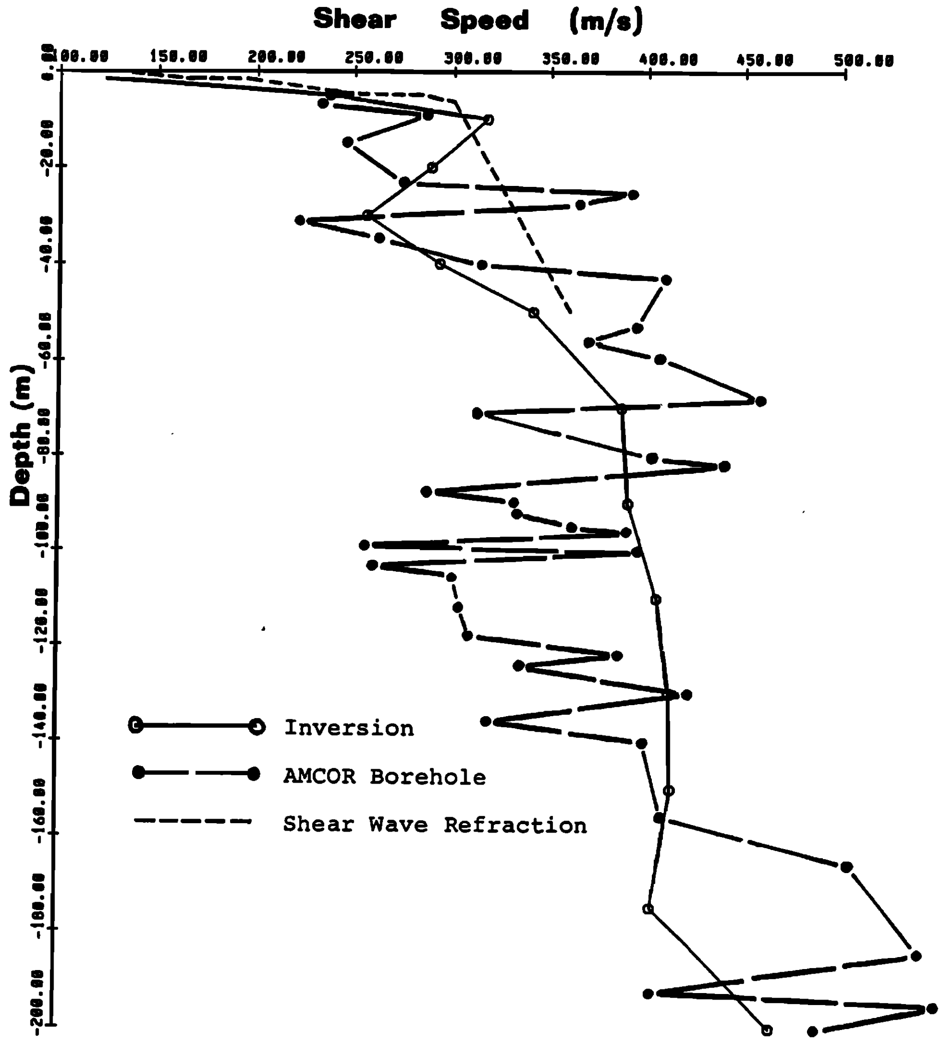

FIG. 8. Comparison of inverted shear wave speed profile from AMCOR6009-303 (converted from shear modulus) with shear wave refraction result (from J. Ewing), and AMCOR borehole reference (converted from bulk density).

similar stratigraphic features to the New Jersey shelf. Richards[27] describes the deeper George's Bank sediments as Pleistocene silty and clayey sands. A complete geological discussion of the COST G-1 well on George's Bank (same location as BSMP experiment) is given by Scholle and Wenkam.[29] The water depth at this site was 51 m, yielding a maximum admittance frequency of 0.156 Hz and a corresponding minimum wavelength of 63.9 m. Thus the minimum resolution depth will again be approximately 20 m. A penetration depth of 200 m and an eigensolution limit of 5 are used, the same as for the AMCOR sites. A comparison between inverted shear wave speed and converted AMCOR borehole 6014 profiles at this George's Bank site is shown in Fig. 10. Due to the large distance (52 km to the SE) to the AMCOR-6014 borehole, the reference should be considered as only a rough indication of the true stratigraphy. Still, there is a rough depth-averaged agreement with the borehole reference. Table AIII (see Appendix) gives the shear modulus inversion result from George's Bank. Notice that the shear modulus increases rapidly in the near surface, reaching 220 MPa at only 10 m. This is indicative of hard, compacted sand with porosities approximately 0.25–0.3.

D. Shallow water carbonates: Key Largo and Miami sites

Two smaller BSMP experiments were conducted in very shallow water south Florida sites near Key Largo and Key Biscayne (Miami). The water depths were 4.5 and 7.6 m, respectively. The sediments were distinctly different than found at the New Jersey shelf sites, being predominantly soft carbonate muds and sands in the near surface, with much harder semilithified basements at depths of only 6 to 8 m. There is little quantitative geotechnical information available, although some descriptive sedimentological studies have been performed in this area (Enos and Perkins[30]). Quantitative shallow water carbonate sedimentary parameters are available from both laboratory and *in situ* tests performed on sediments from the Andros Platform, Bahamas by Badiey *et al.*[31] Enos and Perkins describe the Key Largo site as 4.5–8 m of Holocene carbonate muds and coralline debris overlying semilithified, fossiliferous Pleistocene limestones. They also give measured porosities for the *surficial* carbonate muds as 50%–65%. Badiey *et al.* give measured porosities for carbonate sands as 40%–55%. Due to

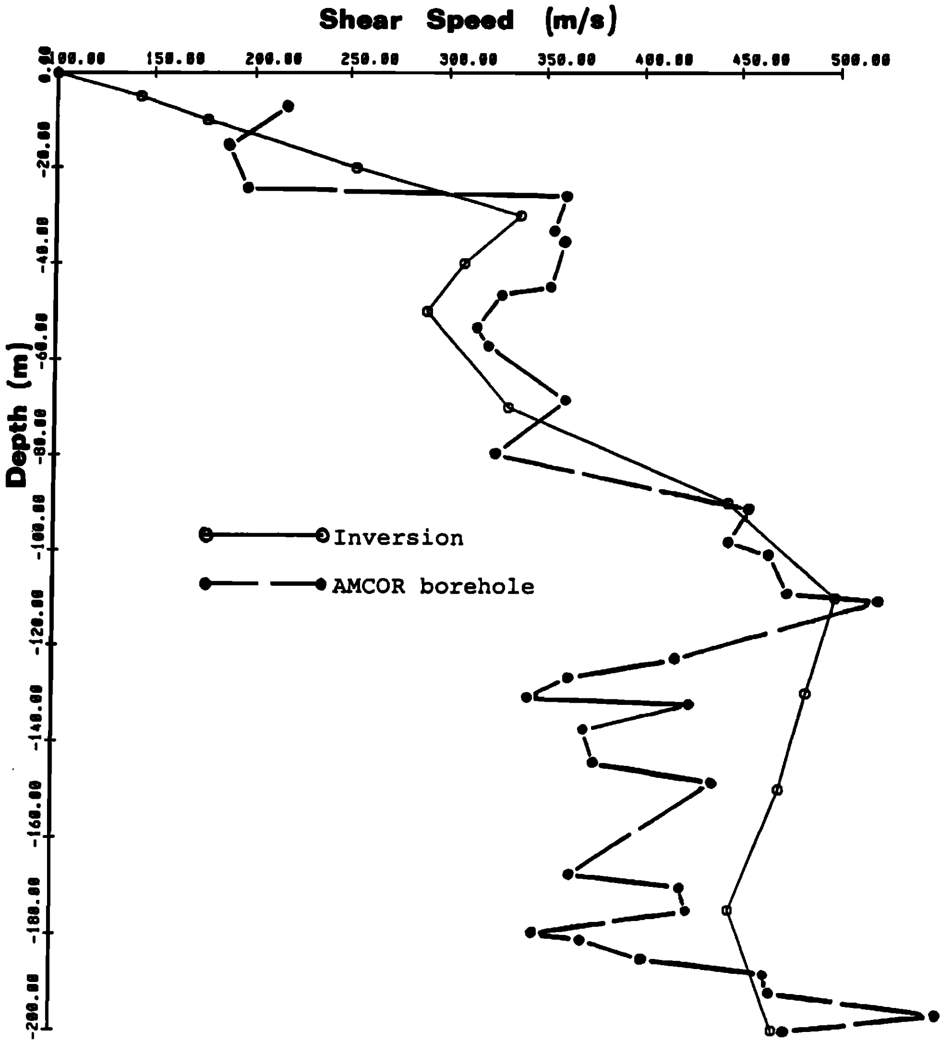

FIG. 9. Comparison of inverted shear wave speed profile from AMCOR6010-87-303 (converted from shear modulus) with AMCOR borehole reference (converted from bulk density).

the shallow waters, the admittance frequency maxima are much larger (> 350 mHz) than in previous examples, resulting in much improved resolution in the near surface layers (minimum resolution depth ≈ 2 m). Due to the presence of hard basement layers the depth penetration is limited. Also, both sites are somewhat sheltered from the open Atlantic ocean swell, so the low-frequency pressure spectrum is greatly reduced. The Miami result only is given, as the Key Largo result is similar.

The Miami experiment is interesting because it was the first successful deployment of the new Guralp CMG-3 ULF seismometers. The shear modulus inversion result for this Miami site is given in Table AIV (see Appendix). The top 6 m of sediments approximates a porosity $= 0.5$ soft carbonate sediment, with a hard, semilithified basement of Pleistocene sediments below 6 m. Due to the close proximity of modern coral reefs, it is also thought possible that this hard basement is a fossilized coral reef. Below 14 m the inversion predicts a softer sediment layer of porosity $\approx 35\%$, indicative of sandy sediments.

VI. DISCUSSION AND CONCLUSIONS

The following characteristics and conclusions can be drawn from the experiments and methods described here.

(i) The method of seabed shear modulus inversion using surface gravity wave-induced seabed motion can determine the magnitude and depth-averaged structure of sediment shear modulus with reasonable accuracy. This follows from direct comparisons of the BSMP results with sedimentary reference data taken from corings and shear wave refraction experiments. Uncertainty bounds on the shear modulus results of $\pm 30\%$–45% are due to mapping of small experimental uncertainties through the inverse calculation.

(ii) Using semiempirical marine sediment models, profiles of porosity, bulk density, shear-wave speed, and compressional wave speed can be extracted from the shear modulus profile. Just as there is agreement between the shear modulus inversion and sedimentary references, there is also agreement with references among these secondary parameters.

(iii) The depth resolution limit in the final shear modulus profile is no less than 20% of the shortest wavelength available in the input data, and occurs in the near-surface layers. Resolution decreases with sediment depth. Due to resolution degradation, the maximum penetration of this BSMP method is approximately 1/2 the longest wavelength available in the input admittance data. Under typical continental shelf conditions (AGS site), these limits correspond

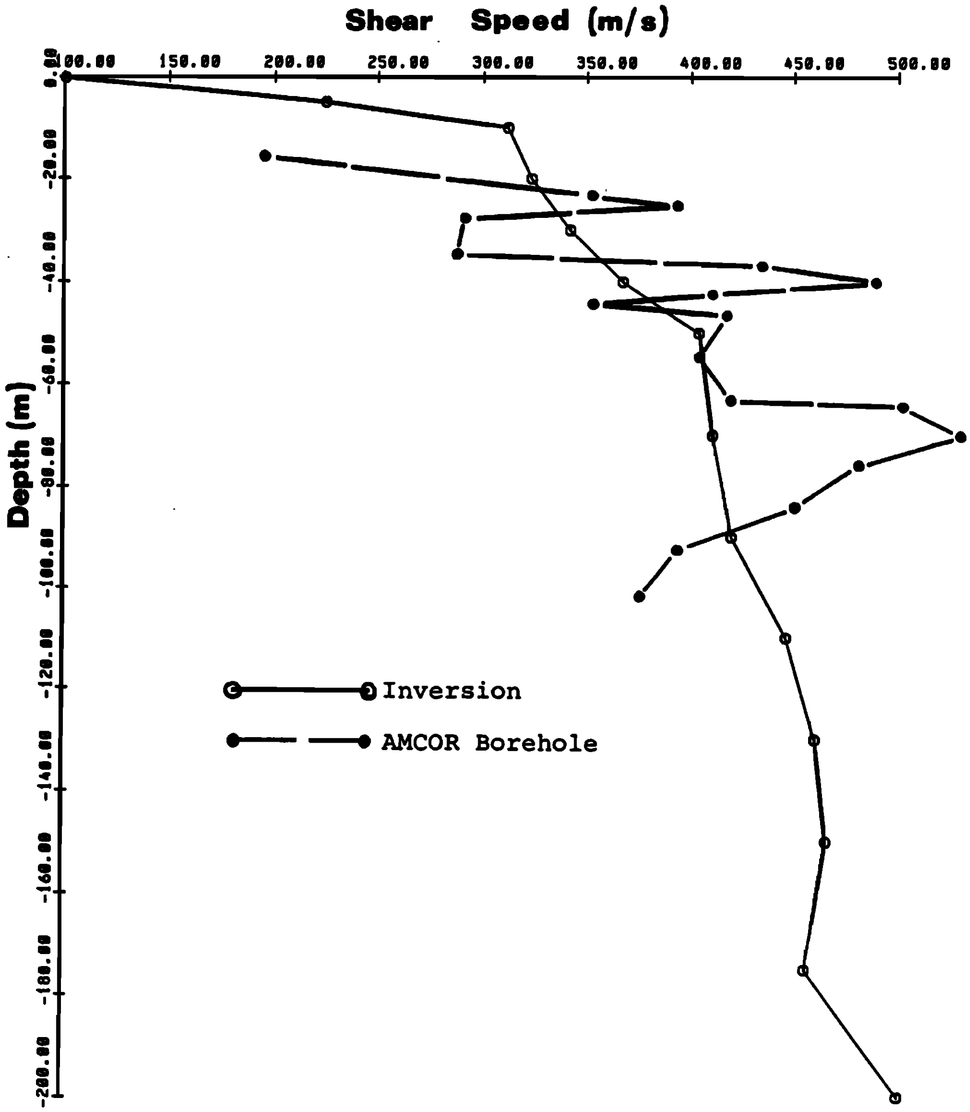

FIG. 10. Comparison of inverted shear wave speed profile from George's Bank (converted from shear modulus) with AMCOR borehole 6014 reference (converted from bulk density). AMCOR 6014 borehole is located 52 km SE of experiment site.

to a minimum resolution of 3 m and a maximum penetration of 100 m.

(iv) In deeper water (> 50 m), the higher frequency waves (140–330 mHz) necessary to resolve finer details in the shear modulus structure near the seabed surface were absent from the coherent admittance data sets. This limitation is imposed by the nature of surface gravity waves, not by a design fault. This cutoff occurs when the water wavelength is approximately 1.3 times the water depth.

(v) The low-frequency limit to coherent admittance data seems to be set by a decrease in surface gravity wave energy below approximately 50 mHz, which causes a corresponding reduction in seabed motion. Typical seismometer designs were limited to frequencies above 30 mHz due to rising internal noise levels at ultra low frequencies.

(vi) With the present BSMP instruments under typical continental shelf conditions, this method is limited to water depths of 300 m or less. This is due to the combination of wave-induced pressure attenuation with depth and a lack of significant water wave energy below 30 mHz. In sheltered waters without open ocean *swell* (50–125 mHz) energy, the BSMP method is limited to water depths of 40 m or less. With much improved instruments (notably seismometers) numerical simulations show that deep ocean (> 2000 m) applications are possible, although with degraded vertical resolution.

ACKNOWLEDGMENTS

This work was supported under several U.S. Office of Naval Research Contracts between 1985–1990. The authors are grateful for this support and the encouragements provided by Dr. Raymond Fitzgerald and Dr. Marshall Orr (Code 1125 OA). The authors also wish to acknowledge the skill and labor of Altan Turgut, Mohsen Badiey, Chuck Abbott, Tom Nye, Dean Goodman, Koichi Ando, and Andy Rogers throughout the evolution of the BSMP system.

APPENDIX

This Appendix contains tabulated sedimentary profile information (Tables AI–AIV) from four other sites described in Sec. VI. See Table I for experimental locations.

TABLE AI. Sediment properties calculated from shear modulus inversion of AMCOR 6009, BSMP 303.

Depth (m)	Shear modulus (MPa)	Density (kg/m^3)	Porosity	Shear speed (m/s)	Comp. speed (km/s)
5.0	116.0	2230.0	0.256	228.0	1.86
10.0	261.0	2340.0	0.193	334.0	2.04
20.0	159.0	2120.0	0.326	273.0	1.76
30.0	141.0	2030.0	0.383	263.0	1.69
40.0	180.0	2060.0	0.363	296.0	1.73
50.0	243.0	2110.0	0.331	339.0	1.79
70.0	323.0	2150.0	0.310	388.0	1.85
90.0	316.0	2110.0	0.335	388.0	1.82
110.0	344.0	2100.0	0.338	405.0	1.82
130.0	356.0	2080.0	0.348	413.0	1.82
150.0	361.0	2070.0	0.358	418.0	1.81
175.0	338.0	2030.0	0.383	408.0	1.78
200.0	464.0	2100.0	0.339	470.0	1.87

TABLE AII. Sediment properties calculated from shear modulus inversion of AMCOR 6010-87, BSMP 303.

Depth (m)	Shear modulus (MPa)	Density (kg/m^3)	Porosity	Shear speed (m/s)	Comp. speed (km/s)
5.0	35.4	1860.0	0.483	138.0	1.56
10.0	64.6	1960.0	0.428	182.0	1.61
20.0	142.0	2090.0	0.343	260.0	1.74
30.0	230.0	2170.0	0.295	326.0	1.83
40.0	201.0	2090.0	0.342	310.0	1.76
50.0	182.0	2030.0	0.380	299.0	1.71
70.0	224.0	2050.0	0.371	331.0	1.74
90.0	415.0	2180.0	0.287	436.0	1.91
110.0	570.0	2240.0	0.253	504.0	2.01
130.0	554.0	2210.0	0.270	501.0	1.98
150.0	514.0	2170.0	0.294	487.0	1.94
175.0	425.0	2100.0	0.339	450.0	1.85
200.0	433.0	2090.0	0.348	455.0	1.85

TABLE AIII. Sediment properties calculated from shear modulus inversion of George's Bank site, Far digital BSMP.

Depth (m)	Shear modulus (MPa)	Density (kg/m^3)	Porosity	Shear speed (m/s)	Comp. speed (km/s)
5.0	112.0	2210.0	0.268	225.0	1.83
10.0	224.0	2300.0	0.216	312.0	1.97
20.0	232.0	2220.0	0.262	323.0	1.89
30.0	257.0	2200.0	0.278	342.0	1.87
40.0	297.0	2200.0	0.278	368.0	1.88
50.0	363.0	2220.0	0.264	404.0	1.93
70.0	368.0	2180.0	0.288	411.0	1.89
90.0	381.0	2160.0	0.303	420.0	1.88
110.0	433.0	2170.0	0.298	447.0	1.90
130.0	459.0	2160.0	0.303	461.0	1.91
150.0	467.0	2140.0	0.312	467.0	1.90
175.0	440.0	2110.0	0.335	457.0	1.86
200.0	539.0	2140.0	0.312	501.0	1.93

TABLE AIV. Sediment properties calculated from shear modulus inversion of Miami site, Guralp seismometers.

Depth (m)	Shear modulus (MPa)	Density (kg/m^3)	Porosity	Shear speed (m/s)	Comp. speed (km/s)
1.5	15.5	1820.0	0.512	92.4	1.53
3.0	18.6	1770.0	0.541	103.0	1.52
4.5	28.2	1830.0	0.502	124.0	1.54
6.0	121.0	2220.0	0.267	233.0	1.84
8.0	318.0	2400.0[a]	0.157[a]	364.0[a]	2.16[a]
10.0	333.0	2380.0[a]	0.165[a]	374.0[a]	2.14[a]
12.0	287.0	2330.0[a]	0.195[a]	350.0[a]	2.04[a]
15.0	154.0	2150.0	0.305	268.0	1.79
20.0	123.0	2050.0	0.370	245.0	1.70
25.0	163.0	2100.0	0.340	279.0	1.75
30.0	207.0	2140.0	0.315	311.0	1.80
35.0	226.0	2140.0	0.313	324.0	1.81
42.0	283.0	2180.0	0.290	360.0	1.86

[a] Sediment is semilithified in these layers, and thus calculation of density, porosity, and acoustic speeds from Eqs. (5)–(17) is inaccurate. Acoustic speeds shown are lower limits to true speeds.

[1] T. Yamamoto, H. L. Koning, H. Sellmeijer, and E. Van Hijum, "On the response of a poro-elastic bed to water waves," J. Fluid Mech. **87**, 193–206 (1978).

[2] T. Yamamoto, "On the response of a Coulomb damped poro-elastic bed to water waves," Marine Geotech. **5** (2), 93–130 (1982).

[3] T. Yamamoto, "Propagator matrix for continuously layered porous seabeds," Bull. Seism. Soc. Am. **73**, 1599–1620 (1983).

[4] T. Yamamoto and T. Torii, "Seabed shear modulus profile inversions using surface gravity (water) wave-induced bottom motion," Geophys. J. R. Astron. Soc. **85**, 413–431 (1986).

[5] R. D. Stoll, G. M. Bryan, R. Flood, D. Chayes, and P. Manley, "Shallow seismic experiments using shear waves," J. Acoust. Soc. Am. **83**, 93–102 (1988).

[6] T. Brocher and J. I. Ewing, "A comparison of high-resolution seismic methods for determining seabed velocities in shallow water," J. Acoust. Soc. Am. **79**, 286–298 (1986).

[7] H. Bradner, "Probing sea-bottom sediments with micro-seismic noise," J. Geophys. Res. **68**, 1788–1791 (1963).

[8] E. L. Hamilton, H. Bucker, D. Kerr, and J. Whitney, "Velocities of compressional and shear waves in marine sediments determined in situ from a research submersible," J. Geophys. Res. **75**, 4039–4050 (1970).

[9] F. B. Jensen and H. Schmidt, "Shear properties of ocean sediments determined from numerical modelling of Scholte wave data," in *Ocean Seismo-Acoustics*, edited by T. Akal and J. M. Berkson (Plenum, New York, 1986).

[10] M. Trevorrow, T. Yamamoto, M. Badiey, A. Turgut, and C. Conner, "Experimental verification of seabed shear modulus profile inversions using surface gravity (water) wave-induced seabed motion," Geophys. J. **93** (3), 419–436 (1988).

[11] M. Trevorrow, T. Yamamoto, A. Turgut, D. Goodman, and M. Badiey, "Very low frequency ocean bottom siesmic noise and coupling on the shallow continental shelf," Mar. Geophys. Res. **11** (2), 129–152 (1989).

[12] M. Trevorrow, T. Yamamoto, A. Turgut, and D. Goodman, "Measurements of ambient seabed seismic noise below 1.0 Hz on the shallow U.S. continental shelf," J. Acoust. Soc. Am. **86**, 2318–2327 (1989).

[13] T. Yamamoto, M. Trevorrow, M. Badiey, and A. Turgut, "Seabed porosity and shear modulus inversion using surface gravity (water) wave-induced seabed motion," Geophys. J. Int. **98** (1), 173–182 (1989).

[14] A. Turgut and T. Yamamoto, "Measurement of acoustic wave velocity and attenuation in marine sediments," J. Acoust. Soc. Am. **87**, 2376–2383 (1990).

[15] F. E. Richart, J. R. Hall, and R. D. Wood, *Vibrations of Soils Foundations* (Prentice-Hall, New York, 1970).

[16] G. M. Bryan and R. D. Stoll, "The dynamic shear modulus of marine sediments," J. Acoust. Soc. Am. **83**, 2159–2164 (1988).

[17] D. Anderson and R. Woods, "Comparison of field and laboratory shear

moduli," in *In situ Measurement of Soil Properties* (ASCE, Raleigh, NC, 1975), pp. 69–92.
[18] R. D. Stoll, "Acoustic waves in ocean sediments," Geophysics **42**, 715–725 (1977).
[19] Y. Ohsaki and R. Iwasaki, "On dynamic shear moduli and Poisson's ratios of soil deposits," J. Soils Found. Jpn. Soc. Soil Mech. Found. Eng. **13** (4), 61–73 (1973).
[20] E. L. Hamilton, "Elastic properties of marine sediments," J. Geophys. Res. **76** (2), 579–604 (1971).
[21] W. Menke, *Geophysical Data Analysis: Discrete Inverse Theory* (Academic, New York, 1984).
[22] R. L. Parker, "Understanding inverse theory," Ann. Rev. Earth Planet. Sci. **5**, 35–64 (1977).
[23] S. Coen, "The inverse problem of the shear modulus profile of a layered earth," J. Geophys. Res. **85** (B10), 5364–5366 (1980).
[24] J. S. Bendat and A. G. Piersol, *Random Data: Analysis and Measurement Procedures* (Wiley–Interscience, New York, 1971).
[25] L. Stahl, J. Koczan, and D. Swift, "Anatomy of a shoreface-connected sand ridge on the New Jersey shelf: implications for the genesis of the shelf surficial sand sheet," Geology **2**, 117–120 (1974).
[26] H. J. Miller and C. Dill, *Final Report, Geophysical Investigation of Atlantic Generating Station Site and Offshore Region*, for the Public Service Electric and Gas Company, Newark, NJ (1974).
[27] A. Richards, "Atlantic Margin Coring Project 1976: Preliminary report on shipboard and some laboratory geotechnical data," U.S.G.S. Open File Report 78-123 (1977).
[28] J. Hathaway, C. Poag, P. Valentine, R. Miller, D. Schultz, F. Manheim, F. Kohout, M. Bothner, and D. Sangrey, "U.S. Geological Survey core drilling on the Atlantic shelf," Science **206** (4418), 515–527 (1979).
[29] P. A. Scholle and C. R. Wenkam, *Geologic Studies of the COST Nos. G-1 and G-2 Wells, United States North Atlantic Outer Continental Shelf*, U.S.G.S. Circular 861 (1982).
[30] P. Enos and R. Perkins, "Quaternary sedimentation in south Florida," Geol. Soc. Am. Mem. 147 (1977).
[31] M. Badiey, T. Yamamoto, A. Turgut, R. Bennett, and C. Conner, "Laboratory and in situ measurements of selected geo-acoustic properties of carbonate sediments," J. Acoust. Soc. Am. **84**, 689–696 (1988).